Characterisation of porous materials

Comparison of experimental determination of transport properties to predicted characterization

SFERA II Project	
Solar Facilities for the European Research Area -Second Phase	
Grant agreement number:	312643
Start date of project:	01/01/2014
Duration of project:	48 months
WP13 – Task 3.C	Deliverable 13.7
Due date:	12/2016
Submitted	12/2016
File name:	WP13 – Task 3.C Deliverable 13.7
Version	1
Partner responsible	ETHZ / CNRS
Person responsible	Aldo Steinfeld (ETHZ) / Cyyril Claiot (CNRS)
Author(s):	S. Ackermann, A. Steinfeld, / Mey-Cloutier S., Caliot C / E. Guillot(summary)
Dissemination Level	PU

Executive Summary

The EU-funded research project SFERA II – grant agreement 312643 – aims to boost scientific collaboration among the leading European research institutions in solar concentrating systems, offering European research and industry access to the best research and test infrastructures and creating a virtual European laboratory.

This deliverable is part of the results of the task 3 of the workpackage 13 *Determination of physical properties of CSP materials under concentrated solar irradiation* within the Joint Research Activities.

This workpackage 13 aims to provide a better evaluation of the material behaviour for CSP applications and other fields with similar thermal stress, such as high temperature steels or SiC ceramics, thanks to better or new experimental tests bed and associated theoretical models. These results will lead to help users developing higher performance materials for higher process efficiency.

The task 3 of workpackage 13 is focused on determining the key properties of porous materials for CSP applications, based on both theoretical and experimental methods:

- Determining heat and mass transfer properties .
- Determining physical and chemical surface properties inside the pores.

The work presented covers 2 actions and is presented in 2 parts:

- Comparison of improved numerical methods and new experimental laboratory setup to assess radiative transfer of reticulated porous materials (lead by ETHZ).
- Development of a new solar setup to experimentally determine porous material heat transfer (lead by PROMES-CNRS).

Workpackage 13 overview

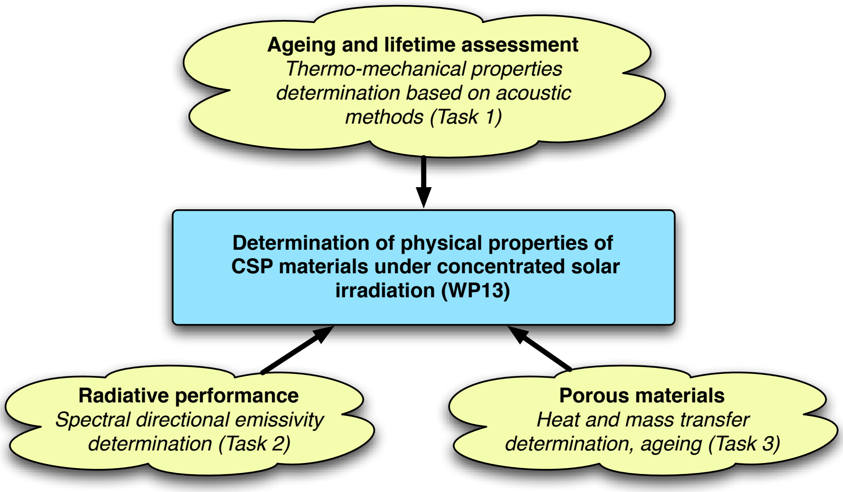

SFERA2 Joint Research Activities : WP13

For completeness, the reader should refer to the other work delivered within the workpackage 13, but also the rest of the project such as WP12 (temperature measurements), WP14 (component qualification) and also the previous project SFERA GA n°228296 such as WP12 task 1 (standardisation activities). http://sfera.sollab.eu/index.php

List of deliverables for SFERA II WP13:

- Task 1, thermo-mechanical properties
  - D13.1: Selected test samples: materials and geometries selected, modelled behaviour.
  - D13.2: Comparison of the modelled behaviour and experimental results from the developed test bed.
- Task 2, radiative properties
  - D13.3: Comparison of experimental determination of emissivity measurements for selected materials between the techniques used by the partners.
  - D13.4: Assessment of experimental measurements of spectral directional emissivity at high temperature.
- Task 3, porous materials properties
  - D13.5: Heat and Mass transport properties of reticulated porous ceramic structures.
  - D13.6: Characterisation of the physical and chemical properties of the surface cavities of porous materials.
  - ➢ D13.7: Comparison of experimental determination of transport properties to predicted characterisation.

Radiative Properties of Reticulated Porous Ceramic Structures

Authors: S. Ackermann, A. Steinfeld, ETH Zurich

Reticulated porous ceramic (RPC) foam-type structures are applied in a solar-driven thermochemical cycle for splitting H_2O and CO_2. The cycle comprises an endothermic step for the reduction of a metal oxide using concentrated sunlight followed by an exothermic step for the oxidation of the reduced metal oxide with H_2O and CO_2 to H_2 and CO. Ceria-based oxides have emerged as highly attractive redox materials because of their relatively high oxygen exchange capacities, fast oxygen-ion transport and high oxidation rates. The redox reactions with pure ceria are represented by:

High-temperature reduction:

$$\mathrm{CeO_2 \rightarrow CeO_{2-\delta} + \frac{\delta}{2} O_2} \tag{1}$$

Low-temperature oxidation with H_2O:

$$\mathrm{CeO_{2-\delta} + \delta H_2O \rightarrow CeO_2 + \delta H_2} \tag{2a}$$

Low-temperature oxidation with CO_2:

$$\mathrm{CeO_{2-\delta} + \delta CO_2 \rightarrow CeO_2 + \delta CO} \tag{2b}$$

where the non-stoichiometry δ denotes the reduction extent. We fabricated RPC foam-type structures with dual-scale porosity: mm-size pores with struts containing micron-size pores. The mm-size pores enable volumetric absorption of concentrated solar radiation and thus effective heat transfer during the reduction step, while the micron-size pores within the struts offer increased specific surface area leading to enhanced reaction kinetics during the oxidation step. A representative 3D rendering of a computer tomography (CT) scan of a RPC sample is shown in **Figure 1**, along with the scanning electron micrograph (SEM) of the strut's cross section.

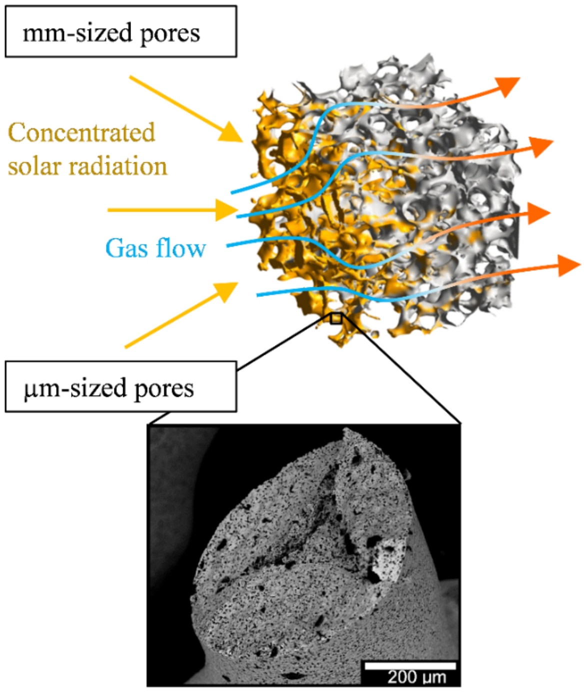

Figure 1. A 3D rendering of a computer tomography (CT) scan of the RPC structure, along with the scanning electron micrograph (SEM) of the strut's cross section. The RPC features dual-scale porosity: the mm-size pores enable efficient volumetric absorption of concentrated solar radiation during the reduction step while the µm-size interconnected pores within the struts provide enhanced kinetic rates during the oxidation step.

Radiation — The design and optimization of solar chemical reactors for effecting the redox cycle demands the development of numerical heat transfer models using accurate radiative properties because radiation is the dominant heat transport phenomena at the reduction temperature . Specifically for RPC structures, the accurate determination of the absorbed and scattered portion of radiation requires the knowledge of the hemispherical reflectivity of ceria r_{CeO_2} as a function of wavelength λ and nonstoichiometry δ:

$$\alpha(\lambda,\delta) = \left(1 - r_{CeO_2}(\lambda,\delta)\right)\cdot\beta$$
$$\sigma(\lambda,\delta) = r_{CeO_2}(\lambda,\delta)\cdot\beta$$

where α is the absorption coefficient, σ the scattering coefficient, and β the effective extinction coefficient. The effective radiative heat transfer properties are computed by applying a collision-based Monte Carlo (MC) ray-tracing method at the pore level using an in-house Fortran code. **Figure 2a** shows β as a function of $d_{m,RPC}$ for various $\varepsilon_{RPC\text{-}single}$. The least-squared correlation is:

$$\beta = \frac{-630.674\cdot\varepsilon_{RPC\text{-}single}^2 - 120.060\cdot\varepsilon_{RPC\text{-}single} + 1229.36}{1000\cdot d_{m,RPC}}\cdot$$

For the porous struts, β_{strut} ~150000 m^{-1}. Because of the high optical thickness, the porous struts are assumed opaque. **Figure 2b** shows Φ as a function of the cosine of the scattering angle, μ_s. A second order polynomial function is least-squared fitted to describe the anisotropic forward and backward scattering and Φ was practically independent of $\varepsilon_{RPC\text{-}single}$ or ppi. The least-squared correlation is:

$$\Phi = 0.63 \cdot \mu_s^2 - 1.43 \cdot \mu_s + 0.79$$

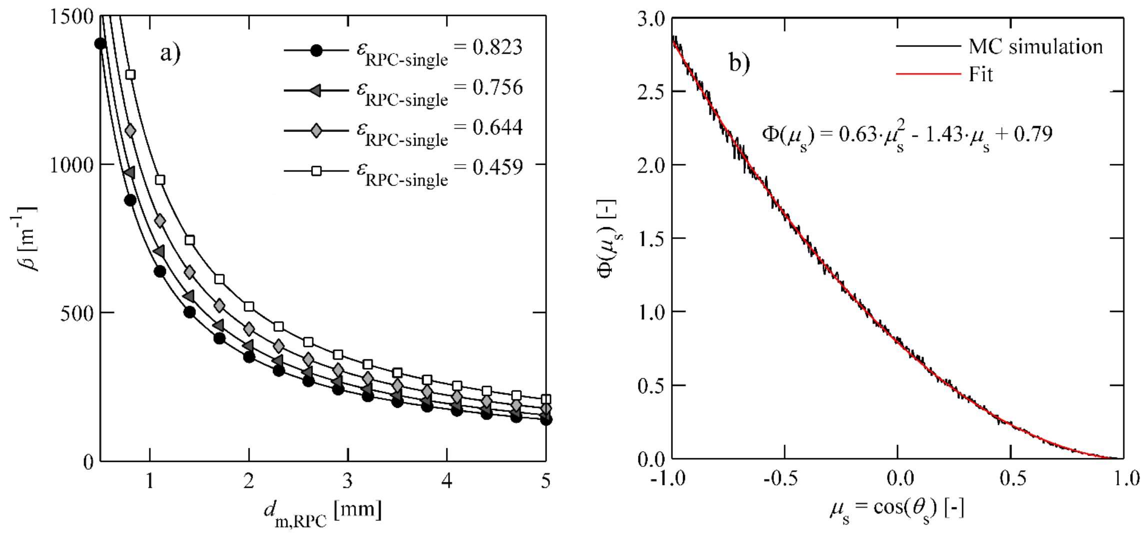

Figure 2. a) Effective extinction coefficient, *β*, as a function of the mean pore diameter for several porosities; b) scattering phase function as a function of the cosine of the scattering angle.

The spectral hemispherical reflectivity of sintered polycrystalline ceria was measured for a wide range of λ and δ relevant for the solar redox cycle. Measurements were performed with a goniometry spectroscopic system shown schematically in **Figure 3.** It consists of: 1) Xe-arc lamp as light source that emits radiation in the range 170 - 3000 nm and approximates a blackbody at 6200 K in the visible range; 2) aspherical Czerny-Turner type double monochromator; 3) mechanical beam chopper to modulate at a frequency of 417 Hz for minimizing background noise; 4) imaging lens; 5) iris to adjust the ray cone angle; 6) mechanical slit; 7) integrating sphere; 8) sample holder; 9) photodetector; 10) lock-in amplifier, and 11) data acquisition system. Three types of photodetectors were used to cover the wide range of wavelengths of interest: a SiC photodiode, a PbS photoconductor and a

InGaAs photodiode covered the ranges 250 – 1000 nm, 800 – 1700 nm and 1000 – 2800 nm, respectively.

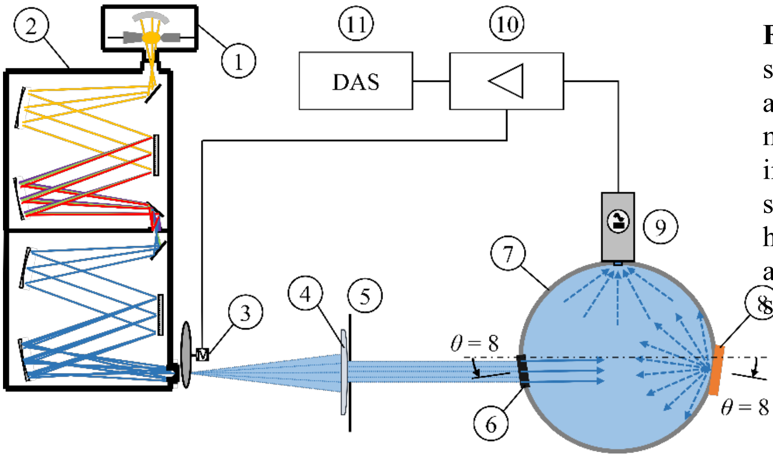

Figure 3. Schematic of the spectroscopic system that consists of a: 1) xenon-arc lamp, 2) double monochromator, 3) chopper, 4) imaging lens, 5) iris, 6) mechanical slit, 7) integrating sphere, 8) sample holder, 9) photodetector, 10) lock-in amplifier, 11) data acquisition system.

Figure 4 shows the mean value of $r_{CeO_2,\lambda}$ as a function of λ for various δ in the range 0 – 0.0377. For δ = 0, $r_{CeO_2,\lambda}$ increases sharply from 0.3 to 0.9 with increasing λ throughout the visible spectrum and remained relatively constant around 0.9 for $\lambda \geq 1000$ nm. This trend is not observed for reduced ceria. Instead, $r_{CeO_2,\lambda}$ increases monotonically over the IR spectrum, reaches a plateau around the 1700–2200 nm band, and decreases for $\lambda > 2200$ nm. For the entire range of wavelengths considered, $r_{CeO_2,\lambda}$ decreases and the sample selectivity diminishes with increasing δ. Note that the colors of each curve shown in Fig. 4 were calculated with the red-green-blue combination of the measured reflectivities and represent the actual sample color.

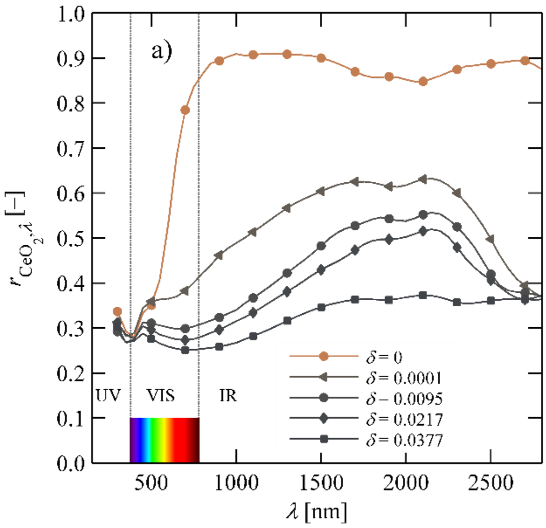

Figure 4. Spectral hemispherical reflectivity of sintered polycrystalline ceria pellets as a function of the wavelength for various nonstoichiometries**.**

References

[1] Ackermann S., Takacs M., Scheffe J., Steinfeld A., "Reticulated porous ceria undergoing thermochemical reduction with high-flux irradiation", *International Journal of Heat and Mass Transfer* 107, pp. 439–449, 2017.

[2] Ackermann S., Steinfeld A., "Spectral hemispherical reflectivity of nonstoichiometric cerium dioxide", *Solar Energy Materials and Solar Cells* 159, pp. 167–171, 2017.

Please also refer to:

SFERA II deliverable D13.5: *Heat and Mass transport properties of reticulated porous ceramic structures.*

S. Ackermann, J.R. Scheffe, J. Duss, A. Steinfeld, Morphological characterization and effective thermal conductivity of dual-scale reticulated porous structures, *Materials* 7 (11) (2014) 7173–7195

Experimental study of ceramic foams used as high temperature volumetric solar absorber and comparison with simulation

Authors: Mey-Cloutier S., Caliot C., Flamant G.[1]
PROMES–CNRS Laboratory (UPR 8521), 7 rue du Four Solaire, 66120 Font-Romeu-Odeillo-Via, France.

Abstract

Volumetric absorbers appear to be a promising technology in order to heat air above 1,000°C to feed combined-cycles (Brayton and Rankine thermodynamic cycles in cascade) for solar thermal electricity production. A test bench was developed and the solar-to-thermal efficiency of reticulate porous ceramics made of SiC with open pores was characterized. Improvements with current state-of-the-art were made by the use of a homogenizer, ensuring quasi-1D incident solar flux irradiation. A new selective porous material was also investigated (Zirconium Diboride, ZrB_2). The lowest porosity values of our samples led to better performances. The performances of the selective absorbers were similar to the SiC absorbers but they showed lower thermal emission losses (at 4.95μm). These results were compared to a reference model which delivered trends with an acceptable accuracy.

Objectives

Recommendations on geometrical characteristics that favour high thermal efficiency can be found in previous articles: Chavez and Chaza (1991) concluded that RPC with high porosity and low PPI would lead to higher solar-to-thermal efficiencies and higher temperatures; Fend and co-authors (Fend et al., 2004) concluded that to intensify convective exchange inside RPC structure one should consider high values of PPI. Both results appear to be contradictory, but the first one (high porosity and low PPI) will allow the solar radiation to penetrate deeper inside the porous structure, whereas the second one (high PPI) will lead to high heat transfer coefficient between air flow and solid structure. In front of these two opposite results, the present work studied both types of foam absorbers to find which characteristics would lead to the best performances. Kribus and co-authors (Kribus et al., 2014) said that optimizing the geometry of volumetric solar receivers is a key step to reach the high efficiency high temperature performances, as variation in geometrical properties led to opposite variation between convective and radiative properties. Thus, the proposed experiments aimed at varying the geometrical properties to determine their influences. Moreover, a material with spectral selectivity (high solar absorptivity and low infra-red emissivity) was also investigated, the Zirconium Diboride, ZrB_2. In addition, a combined heat transfer model of the volumetric receiver at high temperature was developed and validated against the experimental results.

Main experimental results

In this work, a test bench was designed to test volumetric solar absorbers (sample of 5cm diameter, up to 6cm length) submitted to a uniform flux distribution (homogenizer) using a vertical axis solar furnace. The characterization of the setup was conducted to obtain the incident flux density characteristics; calorimetry led to the incident solar power, and fluxmetry led to the flux density distribution. We have experimentally quantified the solar-to-thermal energy efficiency of ceramic foams used as high temperature volumetric solar absorbers. Improvement with current state-of-the-art has been made by the use of a homogenizer, ensuring quasi-1D flux conditions – uniform solar power distribution avoiding hot spots and/or cold spots leading to thermomechanical stress and flow instabilities. Thus, fluxmetry measurements were realized for two purposes: characterization of the solar facility (Gaussian flux distribution at focal point) and validation of the uniform flux operating condition obtained with the homogenizer. The co-current position for the solar incoming power and the air flow rate has been chosen for future comparisons with numerical predictions obtained from approximate models (such as Wu et al., 2011; Mey et al., 2014; Kribus et al., 2014). Several foam samples were tested (silicon carbide SiC from four different suppliers, alumina Al_2O_3, zirconia ZrO_2) covering a range of high porosity (72–92%) and PPI (pores per inch; 5–20 PPI) currently available in the industry, and a new selective material was investigated (ZrB_2). The experimental results for foams were compared to the SiC honeycomb absorber considered to be the reference volumetric receiver.

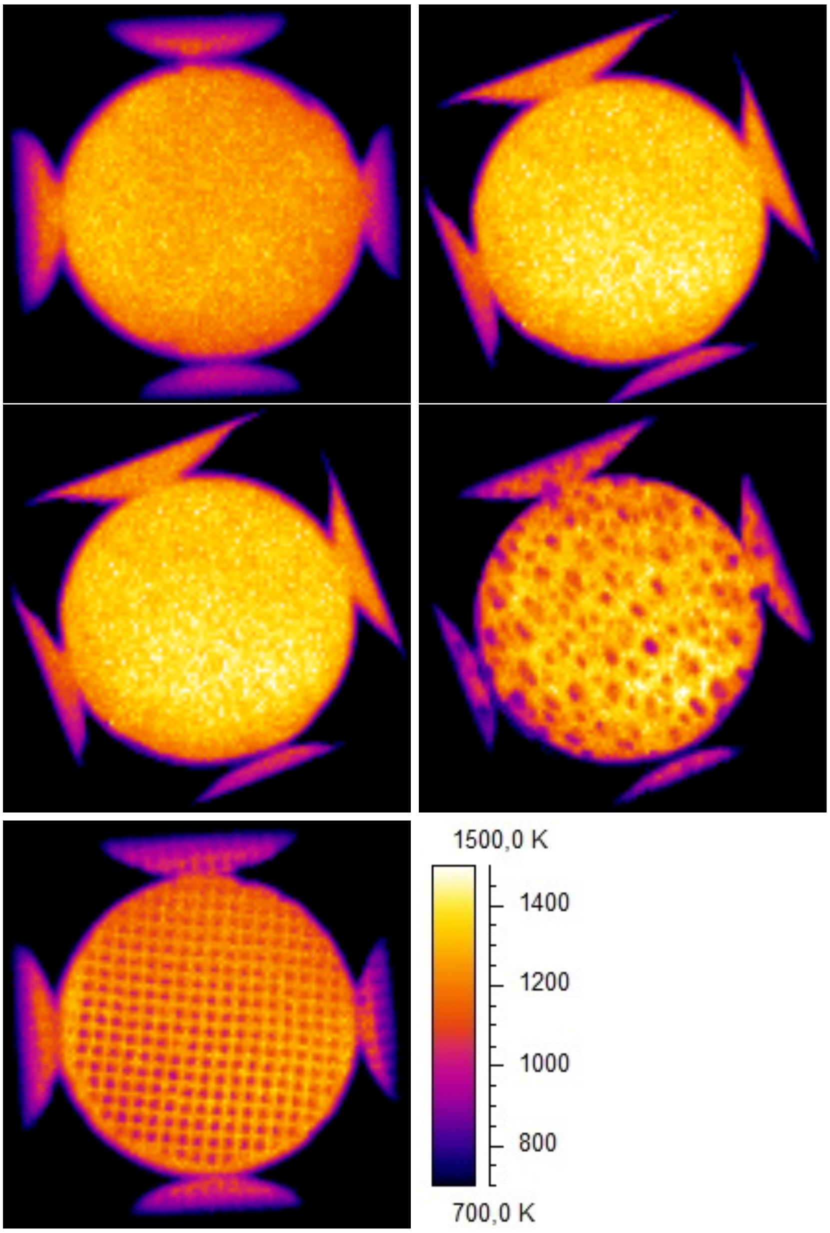

Figure 1: Maps of Blackbody equivalent temperature recorded by the infrared camera: From left to right & top to bottom: ZrB_2, α-SiC (1), Si-SiC (2), $SiC+SiO_2+Al_2O_3$, and SiC honeycombs.

The main result of the experiments is that the random foams with high PPI (meaning a low pore diameter) lead to the best solar-to-thermal performances, probably due to the increase of the convective exchange between the ceramic structure and the air flow. The porosity range of the tested sample was restricted (from 72 % to 88 %), but the lowest porosity values of our samples led to better performances. The performances of the selective absorbers were similar to the SiC absorbers but they showed lower thermal emission losses (at 4.95µm). When low porosity and high PPI foams are used, the optical properties of selective materials are relevant to increase the efficiency of the absorber because of the reduced emission losses. Based on the results of the ZrB2 absorber sample, selective materials should present higher solar absorptivity than the SiC while maintaining low infrared emissivity. This work was published in Solar Energy journal (Mey-Cloutier et al. 2016).

Future experimental works will include to validating the optimal geometrical properties (porosity and PPI) of SiC volumetric absorbers presenting high PPI values. For absorbers with a selective material, the solar absorptivity should be increased and their durability should be evaluated.

Comparison with simulations

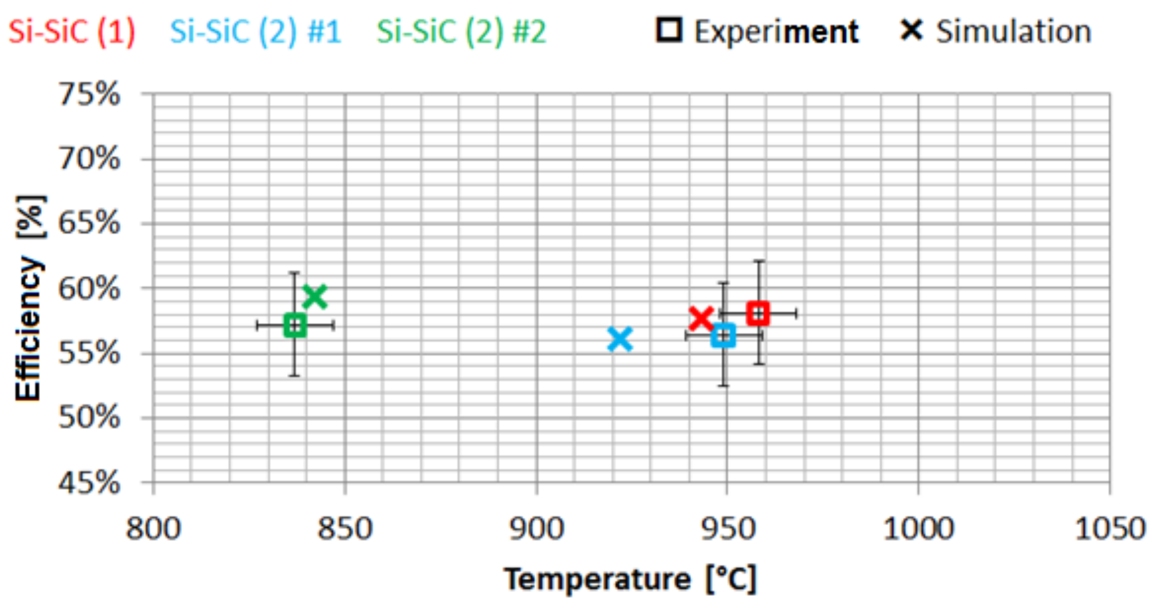

Figure 2: Comparison between experimental and simulation results for the Si-SiC samples. The volumetric receiver solar-to-thermal efficiency and the outlet air temperature are given (with the corresponding confidence intervals for the experiment)

The developed test-bench was used to validate a combined heat transfer model of high temperature porous volumetric receivers containing SiC foams. The model assumes 1D geometry and the foam is modelled as an equivalent porous media with effective properties. The homogenized equations for the flow and heat balance of the fluid (air) and the solid as well as the radiative transfer equation are solved. Correlations are used for effective properties, such as for the Darcy-Forchheimer term of pressure drop, the volumetric convective heat transfer coefficient, the effective conductivity, the effective absorption and scattering coefficients and the phase function. The model was published in Solar Energy (Kribus et al. Solar Energy, 2014). Comparisons between the experimental and the simulation results for different samples of Si-SiC (bought from Engicer SA, Swiss) are presented in Fig. 2. For all the samples, the simulated solar-to-thermal conversion efficiencies are within the confidence interval (+/- 4 %). However, discrepancies were found between the measured and simulated outlet air temperatures with a trend indicating an underestimation of the temperature by the simulation. This bias was attributed to the measurement of the air outlet temperature. Apart from these small discrepancies, the model was found to reproduce the trends with an acceptable accuracy.

References

- Chavez J.M., Chaza C., 1991. Testing of a porous ceramic absorber for a volumetric air receiver. Solar Energy Materials 24, 172–181.
- Fend T., Hoffschmidt B., Pitz-Paal R., Reuter O., Rietbrock P., 2004. Porous materials as open volumetric receivers: Experimental determination of thermophysical and heat transfer properties. Energy 29, 823–833.
- Kribus A., Gray Y., Grijnevich M., Mittelman G., Mey-Cloutier S., Caliot C., Flamant G., 2014. The promise and challenge of solar volumetric absorbers. Solar Energy 110, 463–481.
- Mey S., Caliot C., Flamant G., Kribus A., Gray Y., 2014. Optimization of high temperature SiC volumetric solar absorber. Proceedings of the 19th SolarPACES Conference, Energy Procedia 49, 478–487.
- S. Mey-Cloutier, C. Caliot, A. Kribus, Y. Gray, G. Flamant, 2016. Experimental study of ceramic foams used as high temperature volumetric solar absorber, Solar Energy 136, 226-235.
- Wu Z., Caliot C., Flamant G., Wang Z., 2011. Coupled radiation and flow modelling in ceramic foam volumetric solar air receivers. Solar Energy 85, 2374–2385.

Please also refer to:

SFERA II deliverable D13.6: *Characterization of the physical and chemical properties of the surface of cavities of porous material.*